Res Chem Intermed
https://doi.org/10.1007/s11164-018-3265-8

Pd(OAc)$_2$ immobilized on imine-functionalized microporous covalent triazine polymer as efficient heterogeneous catalyst for Mizoroki–Heck cross-coupling reaction

Velu Sadhasivam[1] · **Mariyappan Mathappan**[1] · **Muniyasamy Harikrishnan**[1] · **Chinnadurai Chithiraikumar**[1] · **Sepperumal Murugesan**[1] · **Ayyanar Siva**[1]

Received: 24 October 2017 / Accepted: 8 January 2018

Abstract A template consisting of Pd(OAc)$_2$ immobilized on imine-functionalized microporous covalent triazine polymer network (Pd/TATAE) was synthesized and found to be an efficient and recyclable heterogeneous solid catalyst for Mizoroki–Heck C–C coupling of styrene with substituted aryl halides under mild reaction conditions and without addition of any ligand or additives. Furthermore, Pd/TATAE could be recycled for nine consecutive cycles with minor loss of catalytic activity. Finally, the Pd/TATAE catalyst showed good catalytic activity with excellent yield of 96 % and high turnover number of 3349.

Keywords Covalent organic polymer · 1,4-Diaminobenzene · Mizoroki–Heck coupling · Palladium catalyst · Shelton test · Triazine

Introduction

Covalent organic polymers (COPs) are a new class of porous crystalline polymeric materials with tailorable [one-dimensional (1D), two-dimensional (2D), and three-dimensional (3D)] structure and different functionalities. This emerging field represents a critical current research area [1]. COPs are micro/mesoporous solid materials that can be synthesized by extending an organic structure via robust covalent linkage of organic building units consisting of light elements such as C, Si,

---

Electronic supplementary material The online version of this article (https://doi.org/10.1007/s11164-018-3265-8) contains supplementary material, which is available to authorized users.

✉ Ayyanar Siva
drasiva@gmail.com

[1] Department of Inorganic Chemistry, School of Chemistry, Supramolecular and Organometallic Chemistry Lab, Madurai Kamaraj University, Madurai, Tamil Nadu 625021, India

O, B, and N only [2]. These porous solid materials possess superior advantages for use in potential applications such as gas storage [3], optical and semiconducting devices [4], electrochemistry [5], drug delivery [6], photocatalysis [7], and sensing [8, 9], among many others, and especially in heterogeneous catalysis [10–12] because of their low density, eclipsed layered porous structure [13], large surface area, tunable properties, thermal and chemical stability, and other functionalities [14, 15]. In addition, porous COP materials are not soluble in any other organic or aqueous solvents and are highly stable in high-boiling solvents.

In recent years, transition-metal catalysis has become an essential tool in organic synthesis [16, 17]. Among transition metals, catalysts containing palladium play a significant role in various cross-coupling reactions such as C–C, C–N, C–O, and C–Se bond formation reactions [18], being widely used for synthetic organic transformations in pharmaceutical and medicinal chemistry [19]. Over recent decades, various homogeneous catalytic systems [20, 21], which always exhibit better activity and high selectivity, have been developed for such organic transformations [22, 23]. However, most homogeneous catalysts suffer from drawbacks such as high-cost phosphine ligands, use of various additives, difficulty in separation, metal leaching, recovery, recyclability, and the toxicity of phosphine ligands. In this regard, Pd catalysts can be heterogenized to overcome such difficulties and make such protocols green.

Recently, a number of studies have focused on incorporation of Pd nanoparticles into various solid supporting materials, including zeolite [24], silica [25], metalorganic frameworks (MOFs) [26], functionalized graphene oxide [27], and COPs to generate heterogeneous catalysts. Moreover, coordination reactions between imine-type (Schiff base) ligands incorporating a variety of metal ions have effectively demonstrated that these are highly stable materials. Thus, over the last few decades, many research groups have been motivated to explore the possibility of using imine-based COFs as excellent platforms for heterogeneous catalysis [16]. Yaghi et al. and Ding et al. first reported imine-based COFs and investigated them for heterogeneous catalysis of C–C coupling reactions [28–30]. In 2011, Farhad Panahi et al. reported palladium nanoparticles supported on a silica-starch substrate (PNP-SSS) as an efficient catalyst for Mizoroki–Heck and Sonogashira coupling reactions [31]. Rahul Banerjee et al. reported synthesis of Pd(II)- and Pd(0)-doped imine-functionalized COF materials and their multifunctional character with catalytic activity in Mizoroki–Heck, Sonogashira, and oxidative biaryl (C–H activation) coupling reactions [32].

Recently, our group successfully synthesized and reported triazine-based microporous covalent imine-functionalized polymers as novel solid supports for palladium (Pd/TATAE)-mediated Suzuki–Miyaura coupling reaction in aqueous medium. In the work reported herein, COP materials were prepared according to our previous literature report [11]. The present study represents an extension of previous work towards the Mizoroki–Heck coupling reaction between styrene and various aryl halides with the aim of achieving good catalytic activity with excellent yield, and high stability in the Mizoroki–Heck coupling reaction, without losing the crystalline structure of the Pd/TATAE catalyst.

Experimental

Materials and instruments

All chemicals and reagents were purchased from commercial suppliers and used without further purification as commercially available unless otherwise noted. All solvents were obtained with laboratory reagent grade. Nitrostyrene, styrene, 4-methylstyrene, bromobenzene, 3-bromopyridine, 2-bromothiophene, and 4-bromobenzaldehyde used in the present study were purchased from Sigma Aldrich. ^{1}H and ^{13}C nuclear magnetic resonance (NMR) spectra were recorded on Bruker (Avance) 300 and 400 MHz NMR instruments with tetramethylsilane (TMS) as internal standard and $CDCl_3$ as solvent. Chemical shifts are given in ppm (δ-scale), and coupling constants are given in Hz. Solution-state ultraviolet–visible (UV–Vis) absorbance was recorded using a JASCO V-630, and solid-state UV diffuse reflectance (DR) spectra were obtained using a JASCO V-670 UV–Vis–near infrared (NIR) spectrometer. The morphology and particle size of the polymerized materials were examined by scanning electron microscopy (SEM) and transmission electron microscopy (TEM) (Bruker). Fourier-transform infrared (FT-IR) spectra were recorded from KBr discs on a JASCO FT/IR-410 spectrometer. Silica gel-G plates (Merck) were used for thin-layer chromatography (TLC) analysis with a mixture of *n*-hexane and ethyl acetate as eluent. Column chromatography was carried out on silica gel (60–120 mesh) using petroleum ether and ethyl acetate as eluent (Scheme 1).

Synthesis of TATAE and Pd/TATAE

Partially crystalline samples of the synthesized compounds of imine-functionalized triazine covalent organic frames such as TATAE and Pd/TATAE were synthesized using our reported procedure (Fig. S1) [11].

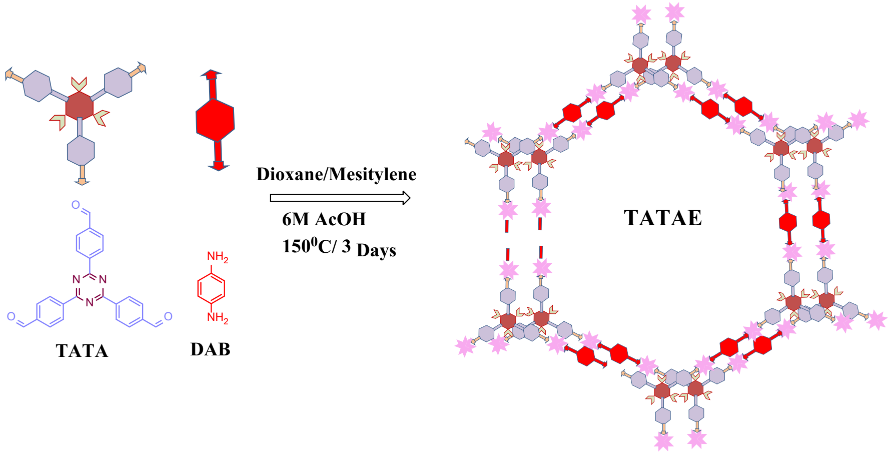

Scheme 1 Schematic representation of synthesis of TATAE and Pd/TATAE (see Fig. S1)

General procedure for Mizoroki–Heck C–C coupling reactions

The potential activity of the newly prepared Pd/TATAE catalyst was analyzed in the Mizoroki–Heck cross-coupling reaction (Scheme 2). Aryl bromide (1 mmol), styrene (1.2 mmol), K_2CO_3 (1.2 mmol), and Pd/TATAE (20 mg) were taken in dimethylformamide (DMF)/water mixture (1:2 ratio, 2 mL), and the mixture was stirred at 70 °C for about 3 h. After reaction completion (monitored by TLC), the reaction mixture was diluted with 5 mL ethyl acetate, then the catalyst was removed by simple filtration using Whatman-40 filter paper. The filtrate was extracted with excess amount of ethyl acetate, then concentrated under reduced pressure. The crude product was further purified by silica gel (60–120 mesh) column chromatography (petroleum ether/ethyl acetate) to afford the corresponding products.

Results and discussion

Characterization of TATAE and Pd/TATAE [11]

The UV-DR spectra of the synthesized materials, viz. TATAE and Pd/TATAE, are shown in Fig. 1, confirming presence of $Pd(OAc)_2$ incorporated on TATAE.

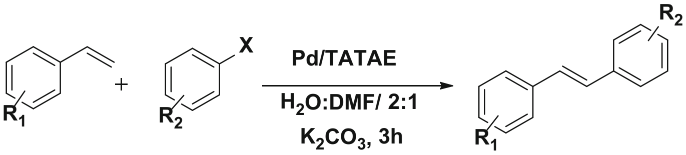

Scheme 2 Mizoroki–Heck C–C cross-coupling reactions

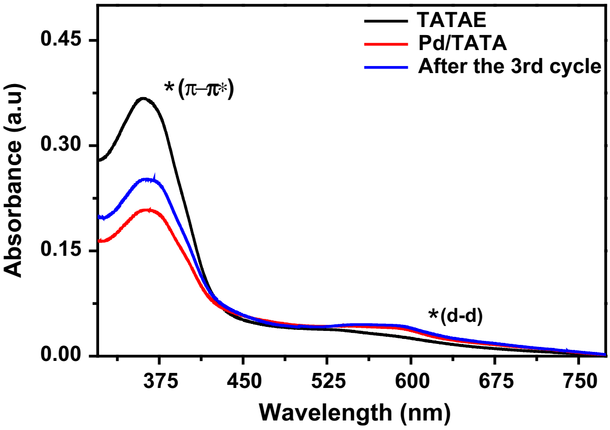

Fig. 1 UV-DRS spectra of TATAE, Pd/TATAE, and after the third cycle

TATAE showed an absorbance band at 362 nm, which can be attributed to π–π^* transition of C=C, C=N. In addition, Pd/TATAE showed a new absorbance band at 590 nm, attributed to *d*–*d* transition of Pd^{2+} metal ions [33]. Thus, the UV-DRS results clearly indicate successful incorporation of $Pd(OAc)_2$ on imine-functionalized microporous covalent triazine polymer. The extended spectrum of the *d*–*d* band is shown in Fig. S2.

The FT-IR spectra of TATAE and Pd/TATAE catalyst matched our previously reported catalyst. The C=N and C=C stretching frequency appeared at 1635 and 1310 cm^{-1}, clearly confirming formation of imine linkages. Furthermore, core triazine ring C=C and C–N stretching appeared at 1514 and 1397 cm^{-1}, respectively. It is suggested that all starting materials were consumed to form the imine-based covalent triazine network, as confirmed by the FT-IR spectrum in Fig. S3. The bands observed at 1709 and 3425 cm^{-1} for TATA and 1,4-diaminobenzene (DAB) can be attributed to free C=O (aldehyde) and primary amine stretching, respectively. Moreover, the free C=O (aldehyde) for TATA and primary amine group stretching band were absent in case of TATAE, indicating that all starting materials were successfully incorporated into the TATAE network. Thus, it is evident from the FT-IR spectrum that both the aldehyde and amine groups were converted into the Schiff base network. Pd/TATAE showed the same absorbance pattern as TATAE, but the C=N stretching absorbance band was shifted by 27 cm^{-1}, while the (υ Pd–N) stretching frequency was observed at 562 cm^{-1} [34], which may reflect possible coordination between $Pd(OAc)_2$ and imine nitrogen atoms. This was further confirmed by measuring the UV-DRS and FT-IR spectra of Pd/TATAE catalyst after the third reuse, revealing no significant changes with respect to the fresh catalyst (Figs. 1, 2). These data clearly suggest that the catalyst retained its structural integrity and stability without any leaching during three cycles under the experimental conditions applied.

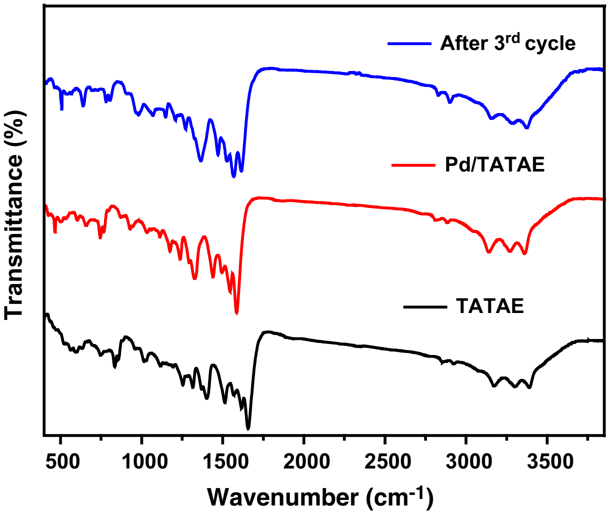

Fig. 2 FT-IR spectra of TATAE, Pd/TATAE, and after the third cycle

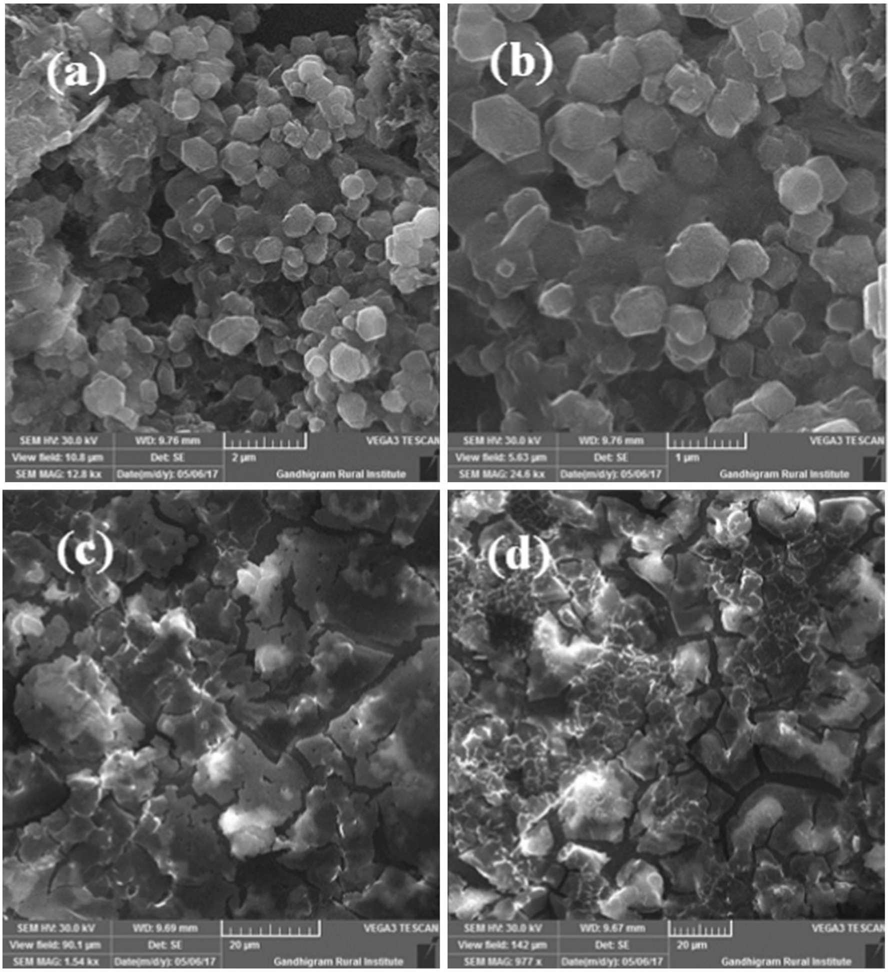

Fig. 3 SEM images and EDS spectrum of **a**, **b** TATAE, **c**, **d** Pd/TATAE, and after the third cycle

The structural morphology of TATAE and Pd/TATAE was confirmed by SEM (Fig. 3), clearly indicating that the TATAE material consisted of porous polymer with crystalline ordered structure. This observation confirms that TATA and 1,4-diaminobenzene led to ordered uniform morphology. After incorporation of $Pd(OAc)_2$ into the TATAE network, Pd/TATAE showed sheet-like morphology. Moreover, the morphological structure changed from porous crystalline ordered to sheet like, indicating that $Pd(OAc)_2$ stacked with each layer of the TATAE network [11]. In addition, the stability of the catalyst under experimental condition was investigated based on SEM images of Pd/TATAE catalyst in fresh state and after three cycles of reuse (Fig. 3), clearly revealing that the morphology of Pd/TATAE retained the sheet-like structure after the Mizoroki–Heck coupling reaction.

The elemental composition of both materials was confirmed by EDS analysis (Fig. 4). The metal content of the Pd/TATAE material was investigated using EDS spectra, confirming presence of C, N, and O elements and Pd^{2+} ions at different points in the microporous imine-functionalized triazine covalent organic framework. The atomic percentage of each element according to the EDS spectrum is presented in Table S1.

Catalytic studies of Pd/TATAE in Mizoroki–Heck C–C coupling reaction

Initially, to check the catalytic activity of the heterogeneous Pd/TATAE in the Mizoroki–Heck coupling reaction (Scheme 2), styrene and bromobenzene were taken as model substrate in presence of Pd/TATAE catalyst for optimization of the reaction condition; the results are summarized in Table 1. Recently, most such coupling reactions have been conducted in aqueous media, attracting a great deal of attention, because water is benign, cheap, nontoxic, more abundant, and environmentally friendly. The Mizoroki–Heck coupling reaction was performed in presence of K_2CO_3 as base in mixture of H_2O/DMF (2:1 ratio, 2 mL) as solvent for 3 h in air atmosphere at 70 °C with yield of 96 % (Table 1, entry 13); only the target product stilbene was observed, while the homocoupled byproduct was not obtained. In addition, no product was obtained (Table 1, entries 1, 2) either in absence of catalyst and base or in presence of TATAE alone. These results clearly demonstrate that Pd/TATAE played a crucial role in the Mizoroki–Heck coupling reaction. The influence of various factors on the reactivity of styrene and aryl halides is discussed below.

When the reaction was conducted with $Pd(OAc)_2$ and $PdCl_2$ instead of Pd/TATAE, yield of 46 and 47 % was observed (Table 1, entries 15, 16). The reaction was optimized with various solvents such as DMF, dimethylsulfoxide (DMSO), ethanol, acetonitrile, H_2O, and DMF/H_2O mixture (Table 1, entries 10–14). Excellent product yield of 96 % was observed in DMF/H_2O (1:2) mixture solvent even at 70 °C. Among these solvents, the DMF/H_2O mixture has high dielectric constant and so is highly soluble and stabilized with the substrate and reactive intermediates compared with other solvents. When the temperature was below

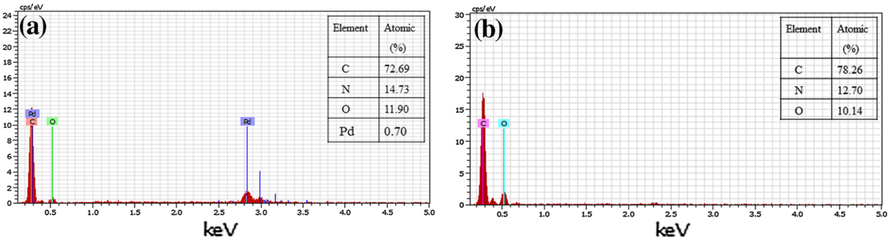

(a)

Element	Atomic (%)
C	72.69
N	14.73
O	11.90
Pd	0.70

(b)

Element	Atomic (%)
C	78.26
N	12.70
O	10.14

Fig. 4 EDS spectrum of **a** Pd/TATAE, **b** TATAE

Table 1 Optimization of Mizoroki–Heck coupling reaction conditions

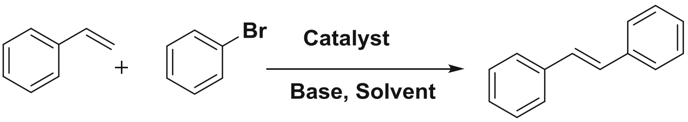

Entry	Catalyst	Solvent	Base	Temp. (°C)	Yield (%)[a]	Conv.[f]
1	–	DMF–H_2O	K_2CO_3	70	–	NR[e]
2	TATAE	DMF–H_2O	K_2CO_3	70	–	NR[e]
3	Pd/TATAE	DMF–H_2O	Na_2CO_3	70	70	70
4[c]	Pd/TATAE	DMF–H_2O	NaOH	70	82	86
5	Pd/TATAE	DMF–H_2O	TEA	70	88	88
6	Pd/TATAE	DMF–H_2O	KOAc	70	45	45
7	Pd/TATAE	DMF–H_2O	K_3PO_4	70	73	73
8	Pd/TATAE	DMF–H_2O	Cs_2CO_3	70	78	78
9	Pd/TATA	DMF–H_2O	Pyridine	70	84	84
10	Pd/TATAE	DMSO	K_2CO_3	90	90	90
11	Pd/TATAE	EtOH	K_2CO_3	70	64	64
12	Pd/TATAE	ACN	K_2CO_3	70	65	65
13	Pd/TATAE	DMF–H_2O	K_2CO_3	70	96	96
14[c]	Pd/TATAE	H_2O	K_2CO_3	90	48	50
15	$PdCl_2$	DMF–H_2O	K_2CO_3	70	47	47
16[b,c]	$Pd(OAc)_2$	DMF–H_2O	K_2CO_3	70	45	48
17[d]	Pd/TATAE	DMF–H_2O	K_2CO_3	70	92	92
18	Pd/TATAE	DMF–H_2O	K_2CO_3	90	96	96
19	Pd/TATAE	DMF–H_2O	K_2CO_3	60	92	92
20[g]	Pd/TATAE	DMF–H_2O	K_2CO_3	70	96	96, 92
21	Pd/C	DMF–H_2O	K_2CO_3	70	73	76
22	Pd/Al_2O_3	DMF–H_2O	K_2CO_3	70	31	37
23	$Pd(PPh_3)_4$	DMF–H_2O	K_2CO_3	70	73	81
24	$PdCl_2(PPh_3)_2$	DMF–H_2O	K_2CO_3	70	61	72
25[h]	Pd/TATAE	DMF–H_2O	K_2CO_3	70	60, 77 84	68, 83, 88

Reaction condition: bromobenzene (1 mmol), styrene (1.2 mmol), base (1.2 mmol), H_2O–DMF solvent (2:1 ratio, 2 mL), catalyst (20 mg Pd/TATAE with Pd content 0.14 wt%, 0.13 mol%), 3 h

[a] Isolated yield based on bromobenzene

[b] 3 mol% $Pd(OAc)_2$

[c] 3 % phenol byproduct formed

[d] Yield of reaction carried out with 1.0 mmol base

[e] NR = no reaction

[f] Determined by GC analysis

[g] Yield of reaction carried out with 20, 15 Pd/TATAE catalyst

[h] Reaction performed with 5, 10, 15 mg catalyst

70 °C (Table 1, entry 19), the product yield decreased to 92 %, whereas increasing the temperature to 90 °C (Table 1, entry 18) had no significant effect on the overall yield. Among different organic and inorganic bases such as K_2CO_3, CH_3COOK, NEt_3, Na_2CO_3, pyridine, K_3PO_4, and NaOH (Table 1, entries 3–9) used for this Mizoroki–Heck coupling reaction, the highest conversion yield of Mizoroki–Heck coupled product was observed for K_2CO_3 (Table 1, entry 13) compared with other bases. In presence of NaOH base, a small amount (3 %) of phenol byproduct formed (Table 1, entry 4). When the amount of base was reduced to 1 mmol, the yield also decreased to 92 %. These results show that the optimum condition for this palladium-catalyzed Mizoroki–Heck coupling was Pd/TATAE (20 mg) catalyst in DMF–H_2O (1:2 ratio, 2 mL) at 70 °C with K_2CO_3 (1.2 mmol) as base for 3 h. Furthermore, the Mizoroki–Heck coupling reaction was also carried out in presence of some commercially available palladium catalysts such as $Pd(PPh_3)_4$, $PdCl_2(PPh_3)_2$, Pd/C, and Pd/Al_2O_3 instead of Pd/TATAE, providing moderate yield of 73, 73, 31, and 61 % (Table 1, entries 21–24). The amount of catalyst was also varied to 5, 10, 15 and 20 mg, resulting in conversions of bromobenzene of 63, 83, 88, and 96 % (Table 1, entry 25).

The reactivity of various substituted aryl halides (X = I, Br) and styrene, including heterocyclic system, was also studied, and the results are presented in Table 2 (entries 1–20) for a wide range of substrates containing both electron-withdrawing and electron-donating groups. In addition, we carried out the Mizoroki–Heck coupling reaction for less reactive aryl chlorides such as chlorobenzene and 4-chlorobenzaldehyde; the reaction proceeded successfully, but with greatly decreased yield (32 %). Moreover, for chloro-substituted derivatives, less amount of starting materials was consumed (Table 2, entries 19, 20). Among the various substrates, the bromobenzene-mediated reaction gave the Heck coupled products in excellent yield of up to 96 % with high turnover number up to 3349 (Table 2, entry 3).

Shelton test

To investigate the heterogeneity of the Pd/TATAE catalyst in our system, we applied the Shelton test for the Mizoroki–Heck coupling reaction of bromobenzene and styrene under the optimized reaction condition (Fig. 5a). During this catalytic reaction, the solid catalyst was filtered from the reaction mixture by simple centrifugation after 30 min (conversion 10.4 %), and the reaction was performed for a further 2.5 h. Thereafter, the reaction mixture was analyzed by gas chromatography, revealing no improvement in product conversion. This result confirms no leaching of Pd into the filtrate solution, suggesting that the Pd/TATAE catalyst was truly heterogeneous in nature and that $Pd(OAc)_2$ was strongly supported on the TATAE network (Table 3).

Reusability test

Recovery and recycling of solid heterogeneous catalysts is one of the major concerns in metal-supported catalysis. Related results are shown in Fig. 5b. Some

Table 2 Water/DMF (2:1)-mediated Mizoroki–Heck coupling reaction catalyzed by Pd/TATAE with various substituents

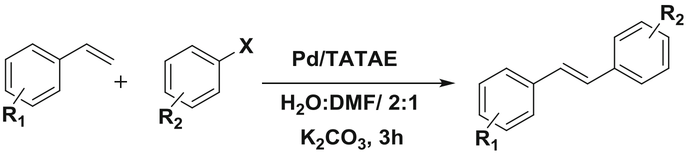

Entry	R_1	R_2	X	Product	Yield (%)[a]	TONs[b]
1	H	CN	Br	**3a**	91	2788
2	H	NO_2	Br	**3b**	85	2373
3	H	H	Br	**3c**	96	3349
4	NO_2	Me	Br	**3d**	82	2155
5	H	NH_2	I	**3e**	93	2995
6	H	CH_2CN	Br	**3f**	88	2523
7	H	3-Pyridine	Br	**3g**	82	2768
8	H	2-Thiophene	Br	**3h**	85	2949
9	CH_3	CH_3	Br	**3i**	90	2721
10	CH_2Br	CH_2Br	Br	**3j**	82	1408
11	H	CHO	Br	**3k**	85	2724
12	H	OH	Br	**3l**	93	2980
13	H	NH_2	Br	**3m**	91	2931
14	H	OMe	I	**3n**	93	2781
15	H	OMe	Br	**3o**	90	2691
16	H	COMe	Br	**3p**	89	2518
17	4-Me	NO_2	Br	**3q**	88	2313
18	NO_2	H	Br	**3r**	84	2344
19	H	H	Cl	**3s**	46	1605
20	H	CHO	Cl	**3t**	32	966

Aryl bromides (1mmol), styrene (1.2 mmol), K_2CO_3 (1.2 equiv), H_2O–DMF solvent (2:1 ratio, 2 mL), Pd/TATAE (20 mg Pd/TATAE with Pd content 0.14 wt%, 0.13 mol%), 70 °C, 3h

[a] Isolated yield based on aryl bromide

[b] TON = mol products/per mol Pd

supported catalysts are not reusable and require a tedious work-up procedure, and after recovery a remarkable decrease in catalyst efficiency is observable. In our catalytic system, reusability was tested using the Mizoroki–Heck coupling reaction of bromobenzene and styrene in presence of (20 mg) Pd/TATAE and K_2CO_3 at 70 °C for 3 h, obtaining yield of 96 %. Afterwards, the catalyst was filtered using Whatman-40 filter paper and washed with water, methanol, ethyl acetate, and excess acetone to remove base and other impurities. Finally, the recovered catalyst was dried in an oven for about 1 h. The catalyst reused in another eight successive cycles under the same reaction condition gave yield of 94, 94, 92, 90, 88, 85, 81, and 77 %

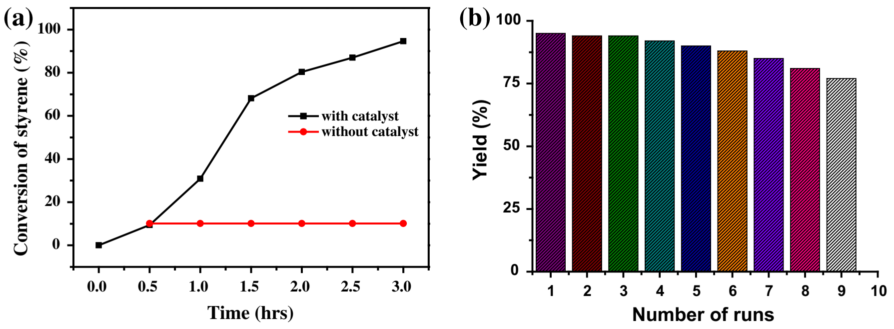

Fig. 5 **a** Effect of reaction time and percentage bromobenzene conversion in Pd/TATAE-catalyzed C–C coupling reactions and hot filtration test for Pd/TATAE catalyst. **b** Reusability of Pd/TATAE catalyst

Table 3 Previously reported catalytic performance of different Pd-incorporated solid supported catalysts in coupling reaction of bromobenzene and styrene

S. no.	Catalyst	Solvent	Base	Temp (°C)	Time (h)	Yield (%)	Ref.
Mizoroki–Heck coupling reactions							
1	Pd-MPTA-1	Water	K_2CO_3	Reflux	6	92	[35]
2	$Pd/CoBDCNH_2$	DMA	NEt_3	90	9	97	[36]
3	CPS-MNPs-NNN-Pd	H_2O–DMF (2:1)	K_2CO_3	90	6	95	[37]
4	PNP-SSS	Water	K_2CO_3	95	12	94	[38]
5	Pd@HSQ	DMF	K_2CO_3	130	2	99	[39]
6	Pd@MCOP	DMSO–H_2O (1:1)	K_2CO_3	90	10	96	[40]
7	MPCS-TI/Pd	DMF–H_2O	NEt_3	110	5	91	[41]
8	Pd(0)-CA	CH_3CN	NEt_3	90	3	94	[42]
9	C_{60}-IL-PdNPs	DMF	NEt_3	120	4	99	[43]
10	Silica-Pd	DMF	K_2CO_3	80	5	82	[44]
11	PEG-Pd(0)	DMF	K_2CO_3	120	6	88	[45]
12	Fe_2O_3/SiO_2/HPG-Pd	DMF	NaOAc	140	12	67	[46]
13	Polymer iminophosphine-Pd	Dioxane	NEt_3	Reflux	5	70	[47]
14	Size-controlled Pd NPs	H_2O	K_2CO_3	100	12	90	[48]
15	Self-assembled Pd-cat	Acetonitrile	Pyridine	100	MW	75	[49]
16	Pd/TATAE	DMF–H_2O	K_2CO_3	70	3	96	Present work

(Fig. 5b), clearly revealing a decrease in catalytic activity and slight loss of product yield after six cycles. In addition, UV–Vis spectroscopy (Fig. S4) of the filtrate solution further confirmed that no absorption peak was observed in the first six cycles, suggesting absence of $Pd(OAc)_2$ in the filtrate solution and that no leaching occurred up to six cycles. However, from the 6th to 10th cycle, new absorbance

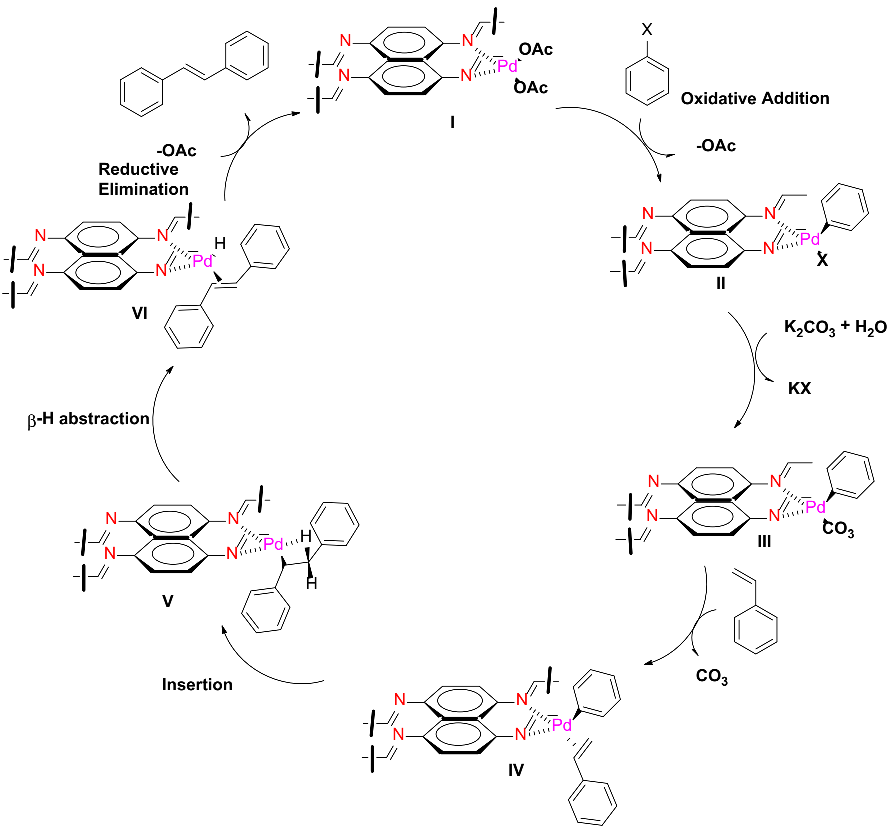

Scheme 3 Plausible mechanism for $Pd(OAc)_2$-catalyzed C–C coupling reactions in the aqueous system

bands appeared at 365 and 310 nm, suggesting minor loss of $Pd(OAc)_2$ by leaching into the filtrate solution.

On the basis of the results presented above, and also in accordance with previous literature reports, a plausible mechanism for the Mizoroki–Heck coupling reaction with the Pd/TATAE catalyst is proposed in Scheme 3. In the first step, oxidative addition of aryl halide with Pd(II) acetate forms Pd complex **II**. In the third step, alkene undergoes insertion reaction, leading to Pd complex **IV**, followed by β-hydrogen abstraction, which results in palladium hydrogen complex **V**. This complex undergoes acetate anion displacement followed by reductive elimination to give the Mizoroki–Heck coupled product.

Conclusions

We designed and synthesized triazine-containing covalent organic frameworks using imine-forming condensation reactions. The covalent triazine framework acted as a good solid support for immobilization of palladium acetate to form Pd/TATAE as a heterogeneous catalyst with efficient catalytic activity in Mizoroki–Heck C–C coupling reactions in mild condition. In addition, the reaction could be performed in absence of any additional stabilizing ligand in very short reaction time. The reaction system showed tolerance toward numerous substituted aryl halides and styrene, giving corresponding products in good to excellent yield. The reaction employs environmentally friendly solvent and additives, inert atmosphere, and ligand-free protocol under mild conditions.

Acknowledgments A.S. and V.S. acknowledge financial support from the Department of Science and Technology, SERB, Extramural Major Research Project (grant no. EMR/2015/000969), Council of Scientific and Industrial Research (CSIR), HRDG (no. 01(2901)/17/EMR-II), New Delhi, and the Department of Science and Technology DST/TM/CERI/C130(G), New Delhi, India.

References

1. Y. Jin, Y. Zhu, W. Zhang, Cryst. Eng. Commun. **15**, 1484 (2013)
2. S.Y. Ding, W. Wang, Chem. Soc. Rev. **42**, 548 (2013)
3. C.J. Doonan, D.J. Tranchemontagne, T.G. Glover, J.R. Hunt, O.M. Yaghi, Nat. Chem. **2**, 235 (2010)
4. S. Wan, J. Guo, J. Kim, H. Ihee, D. Jiang, Angew. Chem. Int. Ed. **120**, 8958 (2008)
5. J. Romero, D.R.S. Miguel, A. Ribera, R.M. Balleste, T.F. Otero, I. Manet, F. Licio, G. Abellan, F. Zamora, E. Coronado, J. Mater. Chem. A **5**, 4343 (2017)
6. A. Rengaraj, P. Puthiaraj, Y. Haldorai, N. Su Heo, S. Hwang, Y. Han, S. Kwon, W. Ahn, Y. Huh, ACS Appl. Mater. Interfaces **8**, 8947 (2016)
7. L. Stegbauer, K. Schwinghammer, B.V. Lotsch, Chem. Sci. **5**, 2789 (2014)
8. A.T.E. Vilian, P. Puthiaraj, C.H. Kwak, S.K. Hwang, Y.S. Huh, W.S. Ahn, Y.K. Han, ACS Appl. Mater. Interfaces **8**, 12740 (2016)
9. J. Yang, L. Yang, H. Ye, F. Zhao, B. Zeng, Electrochim. Acta **219**, 647 (2016)
10. P. Puthiaraj, S. Sung Kim, W. Seung Ahn, Chem. Eng. J. **283**, 184 (2016)
11. V. Sadhasivam, R. Balasaravanan, C. Chithiraikumar, A. Siva, Chem. Sel. **2**, 1063 (2017)
12. L. Li, Z. Chen, H. Zhong, R. Wang, Chem. Eur. J. **20**, 3050 (2014)
13. F.J. Uribe Romo, C.J. Doonan, H. Furukawa, K. Oisaki, O.M. Yaghi, J. Am. Chem. Soc. **133**, 11478 (2011)
14. R. Gomes, P. Bhanja, A. Bhaumik, Chem. Commun. **51**, 10050 (2015)
15. N. Popp, T. Homburg, N. Stockb, J. Senker, J. Mater. Chem. A **3**, 18492 (2015)
16. J.L. Segura, M.J. Manchenoa, F. Zamora, Chem. Soc. Rev. **45**, 5635 (2016)
17. D. Wang, D. Astruc, Chem. Soc. Rev. **46**, 816 (2017)
18. B.M. Choudary, S. Madhi, N.S. Chowdari, M.L. Kantam, B. Sreedhar, J. Am. Chem. Soc. **124**, 14127 (2002)
19. J. Magano, J.R. Dunetz, Chem. Rev. **111**, 2177 (2011)
20. H. Firouzabadi, N. Iranpoor, M. Gholinejad, Tetrahedron **65**, 7079 (2009)
21. H. Pignolet, *Homogeneous catalyst with metal phosphine complexs* (Plenum, New York, London, 1943)
22. R. Imran Khan, K. Pitchumani, Green Chem. **18**, 5518 (2016)
23. H.D. Velazquez, F. Verpoort, Chem. Soc. Rev. **41**, 7032 (2012)
24. A. Thomas, Angew. Chem. Int. Ed. **49**, 8328 (2010)
25. S. Singha, M. Sahoo, K.M. Parida, Dalton Trans. **40**, 7130 (2011)
26. P. Puthiaraj, W. Seung Ahn, Catal. Commun. **65**, 91 (2015)
27. H. Joshi, K. Nayan Sharma, A.K. Sharma, A.K. Singh, Nanoscale **6**, 4588 (2014)
28. A.P. Cote, A. Benin, N.W. Ockwig, M. OKeeffe, A.J. Matzger, O.M. Yaghi, Science **310**, 1166 (2005)
29. F.J. Uribe Romo, J.R. Hunt, H. Furukawa, C. Klock, M.O. Keeffe, O.M. Yaghi, J. Am. Chem. Soc. **131**, 4570 (2009)

30. S.Y. Ding, J. Gao, Q. Wang, Y. Zhang, W.G. Song, C.Y. Su, W. Wang, J. Am. Chem. Soc. **133**, 19816 (2011)
31. A.K. Nezhad, F. Panah, Green Chem. **13**, 2408 (2011)
32. P. Pachfule, M.K. Panda, S. Kandambeth, S.M. Shivaprasad, D.D. Diaz, R. Banerjee, J. Mater. Chem. A **2**, 7944 (2014)
33. K. Mori, M. Kawashima, H. Yamashita, Chem. Commun. **50**, 14501 (2014)
34. S. Jayasree, A. Seayad, R.V. Chaudhari, Org. Lett. **2**, 203 (2000)
35. J. Mondal, A. Modak, A. Bhaumik, J. Mol. Catal. A: Chem. **350**, 40 (2011)
36. F. Ashouri, M. Zare, M. Bagherzadeh, C.R. Chimie **20**, 107 (2017)
37. F. Dehghani, F. Zahra Asadi, F. Panahi, RSC Adv. **6**, 101061 (2016)
38. A. Khalafi Nezhad, F. Panah, Green Chem. **13**, 2408 (2011)
39. N. Moitra, A. Matsushima, T. Kamei, K. Kanamori, Y.H. Ikuhara, X. Gao, K. Takeda, Y. Zhu, K. Nakanishima, T. Shimad, New J. Chem. **38**, 1144 (2014)
40. P. Puthiaraj, K. Pitchuman, Green Chem. **16**, 4223 (2014)
41. B. Movassagh, N. Rezaei, New J. Chem. **39**, 7988 (2015)
42. L. Martın, E. Molins, A. Vallribera, New J. Chem. **40**, 10208 (2016)
43. F. Giacalone, V. Campiscian, C. Calabrese, V. La Parola, L.F. Liotta, C. Aprileb, M. Gruttadauria, J. Mater. Chem. A **4**, 17193 (2016)
44. A.R. Hajipour, P. Abolfathia, F. Mohammadsaleh, RSC Adv. **6**, 78080 (2016)
45. R.F. Alamdari, M.G. Haqiqi, N. Zekri, New J. Chem. **40**, 1287 (2016)
46. L. Zhou, C. Gao, W.J. Xu, Langmuir **26**, 11217 (2010)
47. X. Liu, X. Zhao, M. Lu, J. Organomet. Chem. **768**, 23 (2014)
48. S. Sawoo, D. Srimani, P. Dutta, R. Lahiri, A. Sarkar, Tetrahedron **65**, 4367 (2009)
49. M.N. Nadagouda, V. Polshettiwar, R.S. Varma, J. Mater. Chem. **19**, 2026 (2009)